EGLN1/c-Myc induced Lymphoid-specific helicase inhibits ferroptosis through lipid metabolic gene expression changes

Yiqun Jiang [1,2,3], Chao Mao [1,2], Rui Yang [1,2], Bin Yan [1,2,4], Ying Shi [1,2], Xiaoli Liu [1,2], Weiwei Lai [1,2], Yating Liu [1,2], Xiang Wang [3], Desheng Xiao [5], Fu Zhou [6], Yan Cheng [7], Fenglei Yu [3], Ya Cao [1,2], Shuang Liu [4], Qin Yan [8], Yongguang Tao [1,2,3,4 *]

1 Key Laboratory of Carcinogenesis and Cancer Invasion, Ministry of Education, Xiangya Hospital, Central South University, 87 Xiangya Road, Changsha, Hunan, 410008 China
2 Cancer Research Institute, Central South University, 110 Xiangya Road, Changsha, Hunan, 410078 China
3 Department of Thoracic Surgery, Second Xiangya Hospital, Central South University, Changsha, China
4 Center for Medicine Research, Xiangya Hospital, Central South University, 87 Xiangya Road, Changsha, Hunan, 410008 China
5 Department of Pathology, Xiangya Hospital, Central South University, 87 Xiangya Road, Changsha, Hunan, 410008 China
6 Shanghai Institute of Material Medica, Chinese Academy of Sciences (CAS), 555 Zu Chongzhi Road, Zhangjiang Hi-Tech Park, Shanghai, 201203, China
7 Department of Pharmacology, School of Pharmaceutical Sciences, Central South University, Changsha, Hunan 410078 China
8 Department of Pathology, Yale School of Medicine, New Haven, CT, 06520 U.S.A

* Corresponding author. Y.T. Email: taoyong@csu.edu.cn; Tel. +(86) 731-84805448; Fax. +(86) 731-84470589.

Supplementary Figure legends

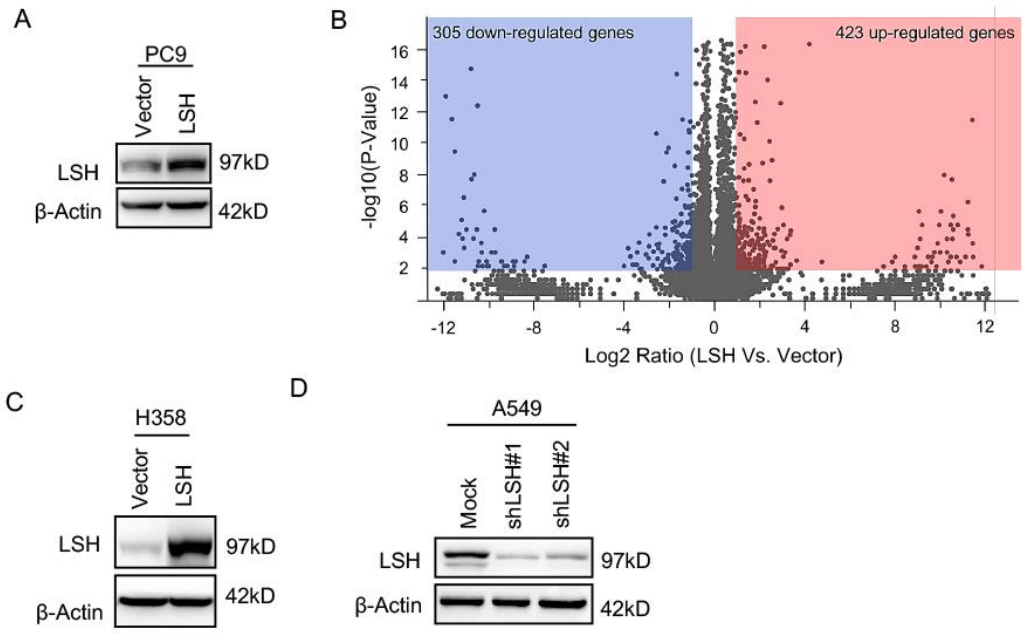

Figure S1. Western blot and RNA-sequencing

(A) Western analysis detected LSH protein level in PC9 cells that were stably transfected with the LSH expression vector. (B) The volcano plot indicates that the two vertical lines are the 2-fold change boundaries, and the horizontal line is the statistical significance boundary. (C) Western analysis detected LSH protein level in H358 cells that were stably transfected with the LSH expression vector. (D) Western analysis detected LSH protein level in A549 cells that were stably knockdown of LSH.

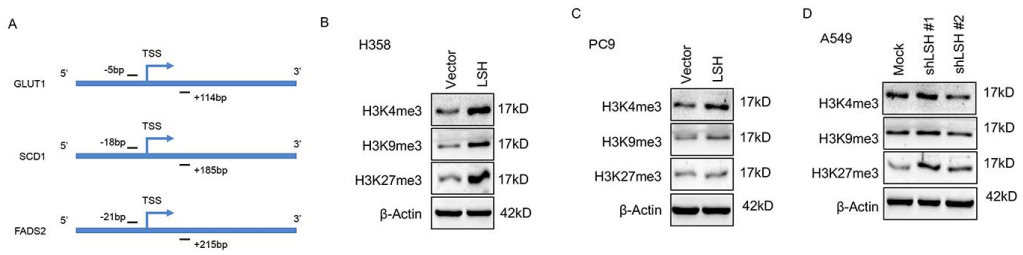

Figure S2. Schematic positions of detected promoters and Western blot of histone modifications in lung cancer cells

(A) Schematic positions of detected promoters. (B-D) Western blot analysis detected Histone modification in the presence of LSH in H358 (B) and PC9 cells (C) and depletion of LSH in A549 cells (D).

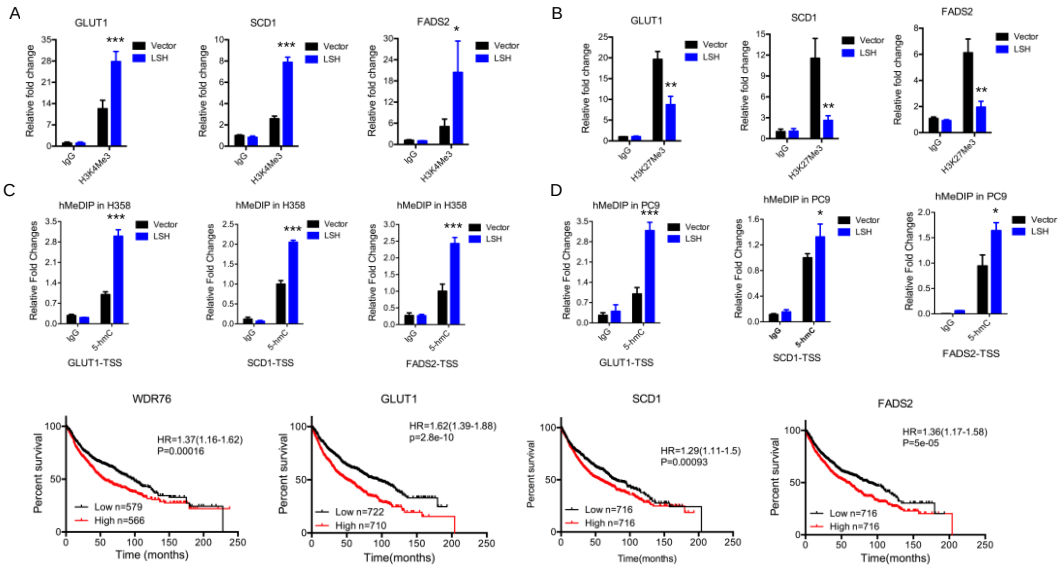

Figure S3. Chromatic changes involve in the regulation of metabolic genes.

(A,B) ChIP analysis of H3K4Me3 (A) and H3K27Me3 (B) at the promoters of GLUT1, SCD1 and FADS2 in H358 cells. (C,D) hMeDIP assay for 5-hmC level at the promoters of GLUT1, SCD1 and FADS2 in H358 (C) and PC9 (D) cells with LSH overexpression. (E) Kaplan-Meier curves for association of WDR76, GLUT1, SCD1 and FADS2 expression with overall survival in lung cancer. * P<0.05, ** P<0.01, *** P<0.001.

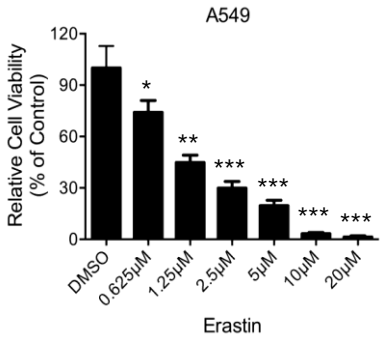

Figure S4. Erastin induces cell death in A549 cells. * P<0.05, ** P<0.01, *** P<0.001.

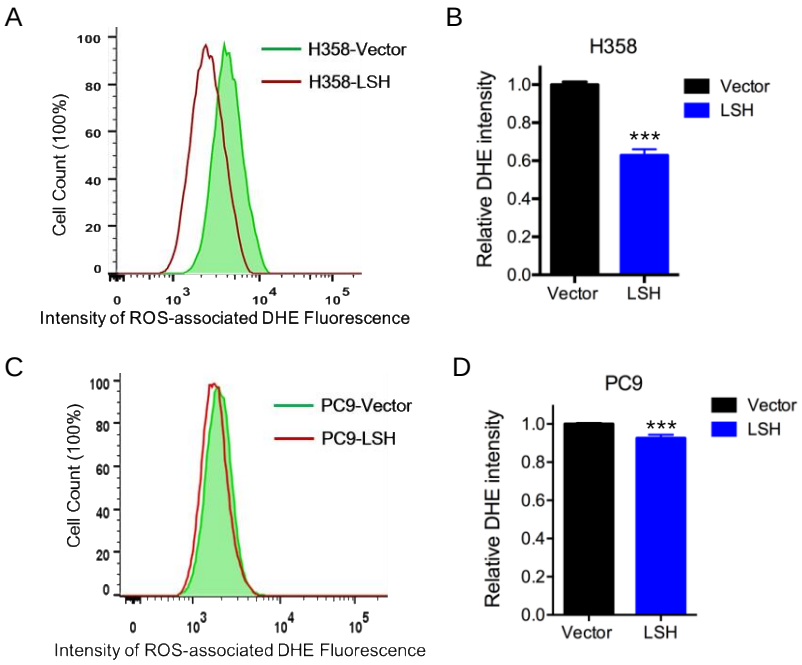

Figure S5. Overexpression of LSH increase the total ROS level.

The total ROS level was measured by DHE-BODIPY staining coupled to flow cytometry in H358 cells that stably overexpressed LSH in a representative experiment (A) and quantitative analysis (B). The total ROS level was measured by DHE-BODIPY staining coupled with flow cytometry in PC9 cells that stably overexpressed LSH in a representative experiment (C) and quantitative analysis (D).

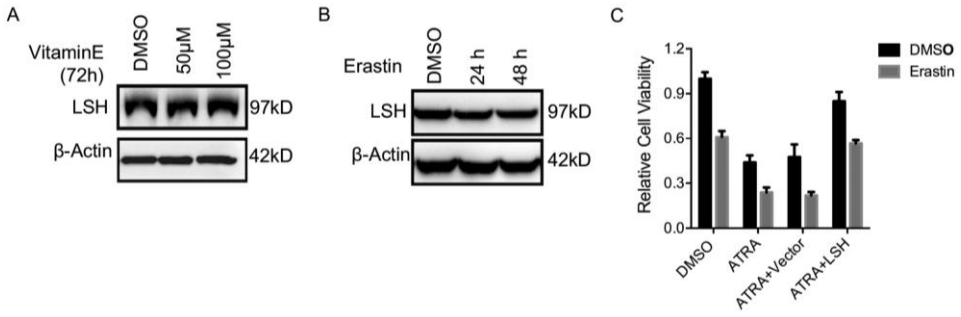

Figure S6. Western Blot and Ferroptosis assay.

(A) Western blot analysis detected LSH expression in the A549 cells in response to Vitamin E for 72 h. (B) Western blot analysis detected LSH expression in the A549 cells in response to Erastin. (C) Erastin induces cell death in A549 cells with the treatment of chemicals as indicated.

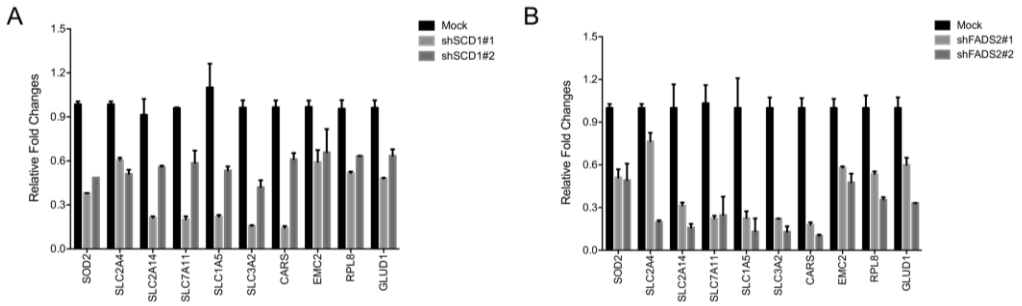

Figure S7. Both SCD1 and FADS2 link with ferroptotic genes. (A) RT-qPCR analysis of ferroptotosis associated genes as indicated after depletion of SCD1. (B) RT-qPCR analysis of ferroptotosis associated genes as indicated after depletion of FADS2.

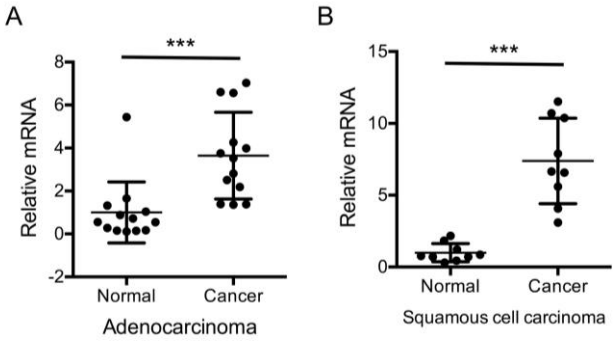

Figure S8. The dot blot analysis, based on a quantitative reverse transcription-polymerase chain reaction (qRT-PCR) analysis expression of LSH in lung adenocarcinoma (A), and in lung SCC (B) for paired lung cancer samples.

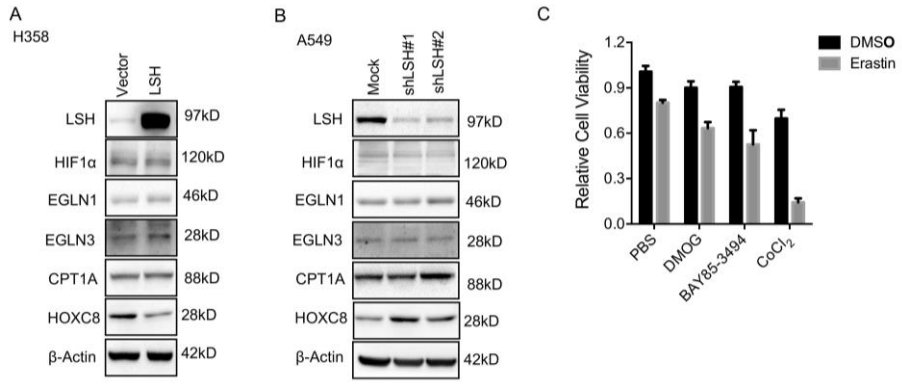

Figure S9. LSH does not affect EGLNs expression.

(A)Western analysis detected the protein levels as indicated in H358 cells after stable expression of LSH. (B) Western analysis detected the indicated protein levels after the depletion of LSH in A549 cells.

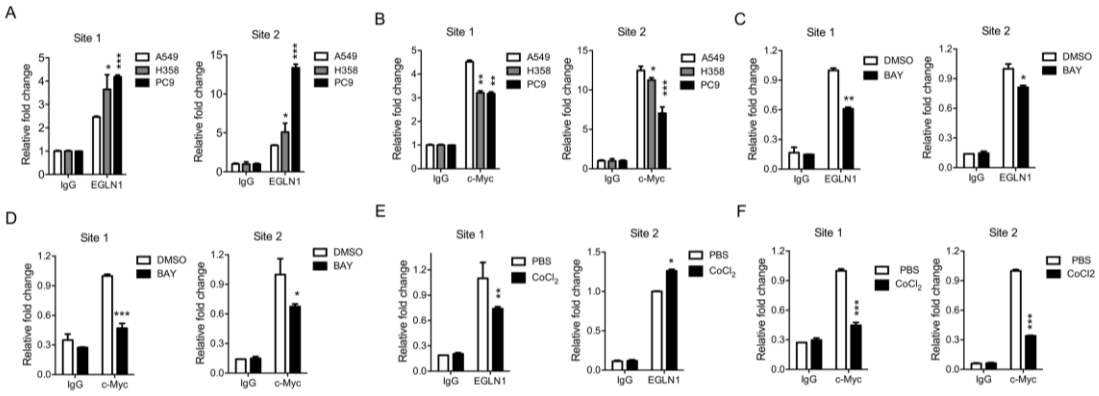

Figure S10. ChIP assays of EGLN1/c-Myc axis in the LSH promoter.

(A, B) ChIP analysis of EGLN1 (A) and c-Myc (B) at the LSH promoter in lung cancer cells. (C-F) ChIP analysis of EGLN1 (C, E) and c-Myc (D, F) at the LSH promoter in A549 cells after treatment with BAY 85-394 (BAY) (C, D) or $CoCl_2$ (E, F). * $P<0.05$, ** $P<0.01$, *** $P<0.001$.

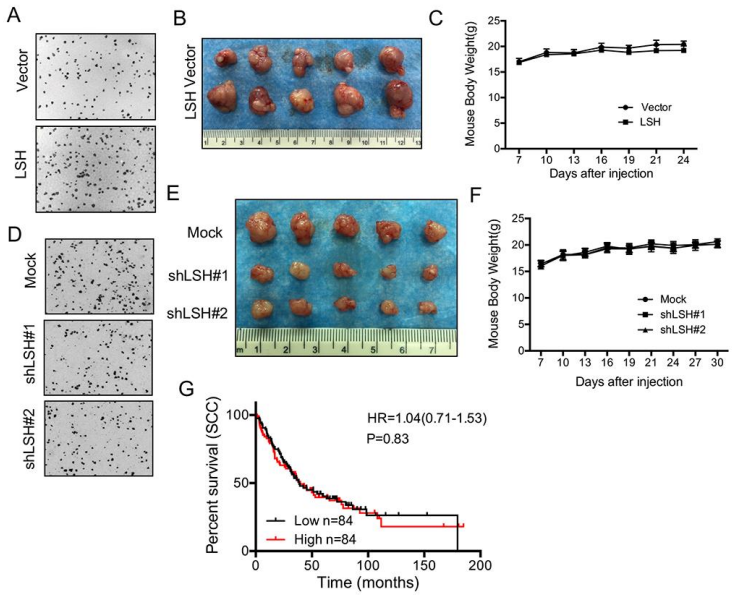

Figure S11. LSH functions as an oncogene in lung cancer *in vitro* and *in vivo*.

(A) A presentive image was shown in growth in soft agar was measured for PC9 cells that stably overexpressed LSH. (B) Tumor formation is shown for nude mice after injection of PC9 cells stably expressing control vector or LSH expression plasmids and (C) Body weight was recorded. (D) A presentive image was shown in growth in soft agar was measured for A549 cells in the depletion of LSH. (E) Tumor formation is shown for nude mice after injection of A549 cells that were stably transfected with two distinct LSH shRNA expression vectors (siLSH#1 and siLSH#2) and control cells (Mock) and (F) Body weights were recorded. (G) Kaplan-Meier curves for overall survival rate of the related samples measured in lung SCCs.

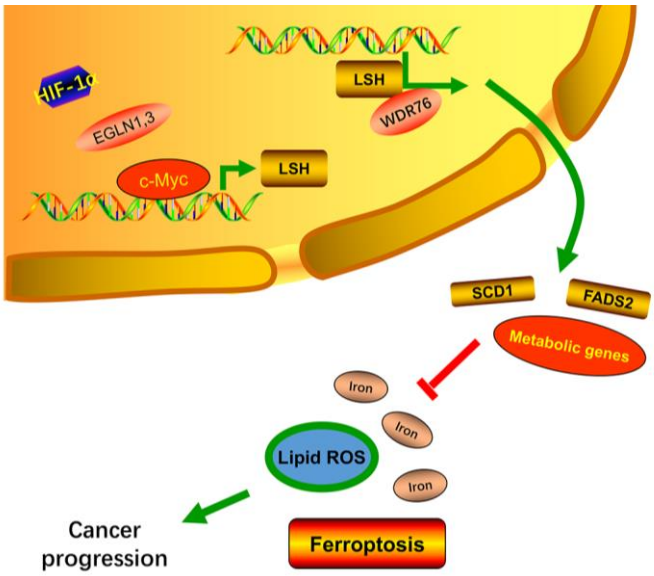

Figure S12. The schematic model of LSH in ferroptosis. Transcription factor c-Myc is induced by EGLN1 to upregulate LSH expression. LSH upregulates metabolic genes including GLUT1, SCD1 and FADS2 through interacting with WDR76. The metabolic genes inhibit the accumulation of lipid ROS and intracellular iron, two surrogate markers of ferroptosis, which in turn promotes cancer progression.

Supplementary Material and Methods

Western blot analysis and Co- Immunoprecipitation (Co-IP) assay

Details of the Western blot analysis were described previously [1]. Cells were harvested, washed twice with ice-cold phosphate-buffered saline (PBS), lysed in radio immunoprecipitation assay (RIPA) buffer and centrifuged at 15,000 × g for 10 min after sonication. The supernatants were collected as whole cell lysates. A quantity of 50 μg of total protein was used for Western blot analysis. For immunoprecipitation experiments, cells were plated overnight in 100 mm^2 dishes (1.5×10^6/dish). A quantity of 1 mg of protein was mixed with 40 μl of Protein A-Sepharose beads (Sigma) in the immunoprecipitation assay buffer (1× PBS, 0.5% Nonidet P-40, 0.5% sodium deoxycholate and 0.1% SDS), incubated at 4°C for 2 h with gentle agitation and centrifuged for 10 min at 2000 rpm for preclearing. The recovered supernatant was incubated with 10 μl of anti-Flag M2 agarose (Sigma) in the presence of 1× protease inhibitors at 4°C overnight with mild shaking. The M2 agarose-precipitated protein complex was recovered by a brief centrifugation followed by three washes with the immunoprecipitation assay buffer. The harvested beads were re-suspended in 30 μl of 2× SDS PAGE sample buffer and boiled for 5 min to release the bound protein. A 20 μg aliquot of cell lysate was used as an input control. The samples were analyzed by Western blot. The antibodies used for Western blot detection were the LSH, WDR76 antibodies.

Quantitative real-time PCR and and RNA sequencing

Cells were harvested with Trizol (Invitrogen). cDNAs were synthesized with SuperScript III (Invitrogen) according to the manufacturer's protocol. Real-time PCR analysis was performed using the Applied Biosystems 7500 Real-Time PCR System, according to the manufacturer's instructions. The reactions were performed in triplicates for three independent experiments: the results were normalized to **β**-actin. The primer sequences used were used in the supplementary Table S1. The mean± SD of three independent experiments was shown.

For RNA sequencing, the total RNA samples are first treated with DNase I to degrade any possible DNA contamination. Then the mRNA is enriched by using the oligo(dT) magnetic beads. Mixed with the fragmentation buffer, the mRNA is fragmented into short fragments. Then the first strand of cDNA is synthesized by using random hexamer-primer. Buffer, dNTPs, RNase H and DNA polymerase I are added to synthesize the second strand. The double strand cDNA is purified with magnetic beads. End reparation and 3'-end single nucleotide A (adenine) addition is then performed. Finally, sequencing adaptors are ligated to the fragments. The fragments are enriched by PCR amplification. During the QC step, Agilent 2100 Bioanaylzer and ABI StepOnePlus Real-Time PCR System are used to qualify and quantify of the sample library. The library products are ready for sequencing via Illumina HiSeqTM 2000. The whole RNA-sequencing process and data analysis was conducted by BGI Tech, Shenzhen, China.

Cell proliferation assay, migration and invasion assay and plate-colony

formation assay.

Details of the cell proliferation assay were described previously [1]. For plate-colony formation assay, cells (2×10^3/mL/well) were seeded into 6-well plates and cultured in RPMI-1640 medium supplemented with 10% FBS. Colonies were fixed with methanol and stained with viola crystalline, then scored using a microscope and Image J software (1.47V, NIH, USA).

The migration assay was described previously [2]. Cells (5×10^5) were seeded onto the upper chamber in 200 μL of serum-free medium; the lower compartment was filled with 0.6 mL of DMEM media supplemented with 10% of FBS. After 24 hours incubation, migrated cells on the lower surface of the filter were fixed and stained using propidium iodide. Cells on the upper side were removed using a rubber scraper. Fluorescent images were obtained. The reported data represents counts of migrated cells. Experiments were performed in triplicates.

For the plate-colony formation assay, cells (2×10^3/ml/well) were seeded into 6-well plates and cultured in RPMI-1640 medium supplemented with 10% FBS. Colonies were fixed with methanol, stained with viola crystallina and scored using a microscope and ImageJ software (1.47V, NIH, USA).

Immunofluorescence assay

Details of the immunofluorescence assays were described previously [1], cells were cultured and fixed in 4% paraformaldehyde for 30 min. To identify the potential presence of LSH and WDR76, cells were incubated with an anti-LSH antibody

(Sigma) and an anti-WDR76 antibody (Active motif) and then with fluorescein isothiocyanate (FITC)-conjugated anti-IgG (Santa Cruz) and Cy3-conjugated anti-IgG (Sigma). To visualize the nuclei, the cells were stained with Hoechst (1:1000). Fluorescent images were observed and analyzed with a laser scanning confocal microscope (Bio-Rad MRC-1024ES).

Chromatin immunoprecipitation (ChIP) assays

ChIP assays were essentially performed as previously described [1] with modifications: 5×10^6 cells were fixed with formaldehyde (1% final volume concertration, Sigma), 10 min at room temperature. Fixation was stopped by addition of 1/10 volume 1.25 M glycine and incubated for 5min at room temperature. The sonication step was performed in a Qsonica sonicator (5min, 20s on, 20s off), and 200 μg of protein-chromatin complex was used for each immunoprecipitation. Antibody-protein complex was captured with preblocked dynabeads protein G (Invitrogen). ChIP DNA was analyzed by qPCR with SYBR Green (Biorad) in ABI-7500 (Applied Biosystems) using the primers specified in Supplemental Table S2. The antibodies used are as followed: LSH (Santa), WDR76 (Sigma) normal mouse IgG(12-371, Millipore).

Measurement of total ROS and Lipid

Details of the procedures were described previously [3, 4]. For total ROS, cells were treated as indicated then trypsinized and resuspended in medium plus 10% FBS, then

4μM Dihydroethidium (DHE, Sigma, Cat.# 37291) was added and incubated for 15min at 37°C, 5% CO_2 and protected from light. Excess DHE was removed by washing the cells twice with pre-warmed PBS. DHE was oxidized to highly red fluorescence ethidium which is proportional to ROS generation and was analyzed using a flow cytometer (Fortessa, BD Biosciences). More than 10 000 cells were analyzed per condition.

For Lipid ROS, cells were treated as indicated, and then typsinezed and resuspended in medium plus 10% FBS, then 10μM C11-BODIPY (Thermo Fisher, Cat# D3861) was added and incubated for 30min at 37°C, 5% CO_2 and protected from light. Excess C11-BODIPY was removed by washing the cells twice with PBS. Oxidation of the polyunsaturated butadienyl portion of the dye results in a shift of the fluorescence emission peak from 590nm to 510nm proportional to lipid ROS generation and was analyzed using a flow cytometer.

Measurement of Iron

Iron Assay Kit (Sigma, Cat.# MAK025) was used to determine the relative ferrous(Fe^{2+}) iron and total iron level in indicated cells. Iron is first released by the addition of Iron Assay Buffer, then to measure ferrous iron, add 5μL of iron assay buffer to each sample and blank well, to measure total iron, add 5μL of Iron Reducer to each of the sample wells. Mix well using a horizontal shaker, and incubate the reaction for 30 min at room temperature. Protect the plate from light during the incubation. Then add 100μL Iron Probe to each well, mix using a horizontal shaker

and incubate the reaction for 60min at room temperature and protected from light. Measure the absorbance at 593nm.

Nude mice and study approval

A xenograft tumor formation was essentially performed as previously described [2]. SCID Mice (Hunan SJA Laboratory Animal Co., Ltd.) were injected with A549 (1×10^6 cells/mouse) or H358 (2×10^6 cells/mouse) cells via mammary fat pad (10 mice/group). Mice with A549 or H358 cells were imaged from dorsal and ventral views every three days. Data were analyzed using Student's t-test; a p value< 0.05 was considered significant.

All procedures for animal study were approved by the Institutional Animal Care and Use Committee of the Central South University of Xiangya School of Medicine and confirm to the legal mandates and federal guidelines for the care and maintenance of laboratory animals.

Immunohistochemistry (IHC) analysis

Lung and related diseases biopsies were validated and obtained from Department of Pathology in Xiangya Hospital. IHC analysis of paraffin sections from lung cancer tissues was described previously [2]. The sections were incubated with antibodies as indicated. The images were surveyed and captured using a CX41 microscope (OLYMPUS, Tokyo, Japan) with the Microscope Digital Camera System DP-72 (OLYMPUS, Tokyo, Japan) and differentially quantified by two pathologists who

were from the Xiangya Hospital, Changsha, China.

LSH and WDR76 were considered positively by nuclear expression. The determination results were obtained from semi-quantitative classification according to 10 or more visual fields (×200). The slides were first scored as 0 (negative), 1 (buff), 2 (pale brown), and 3 (tan). Positive expression of LSH was scored as 0 (negative), 1+ (<10% of positively-staining tumor cells), 2+ (11-50% of positively-staining tumor cells), 3+ (50-75% of positively-staining tumor cells), and 4+ (>75% of positively-staining tumor cells). Both the scores by multiply were regarded as the determination result.

Table S1 RT-PCR primers.

Name	Full Name	Entrez Gene ID	Sequence	Product Size(bp)
LSH(HELLS)	helicase, lymphoid-specific	3070	F: AGAAGGCATGGAATGGCTTAGG R: GCCACAGACAAGAAAAGGTCC	151
FADS1	Fatty Acid Desaturase 1	3992	F: CCAACTGCTTCCGCAAAGAC R: GCTGGTGGTTGTACGGCATA	120
FADS2	Fatty Acid Desaturase 2	9415	F: TGACCGCAAGGTTTACAACAT R: AGGCATCCGTTGCATCTTCTC	98
FADS3	Fatty Acid Desaturase 3	3995	F: CCCTGGTGAACTTTGAAGTGG R: GGAGGTAGGATAAGAAGAAGCGG	111
FADS4(SCD5)	Stearoyl-CoA Desaturase 5	79966	F: GAGGAATGTCGTCCTGATGAGC R: GCCAGGAGGAAGCAGAAGTAGG	114
FADS5(SCD1)	Stearoyl-CoA Desaturase	6319	F: CCTGGTTTCACTTGGAGCTGTG R: TGTGGTGAAGTTGATGTGCCAGC	106
FADS6	Fatty Acid Desaturase 6	283985	F:GAACGTGTCAGGCTTCAAGAA R:CTCATCATGTGAATCCGACGG	159
FADS7	Delta(4)-Desaturase, Sphingolipid 1	8560	F: GAGATCCTGGCAAAGTATCCAGA R: CAAACGCATAGGCCCCAAA	157
GLUT1	Solute Carrier Family 2 Member 1	6513	F: TTGCAGGCTTCTCCAACTGGAC R: CAGAACCAGGAGCACAGTGAAG	113
GLUT3	Solute Carrier Family 2 Member 3	6515	F:GCTGGGCATCGTTGTTGGA R:GCACTTTGTAGGATAGCAGGAAG	123
GLUT4	Solute Carrier Family 2 Member 4	6517	F: CCATCCTGATGACTGTGGCTCT R: GCCACGATGAACCAAGGAATGG	133
GLUT6	Solute Carrier Family 2 Member 6	11182	F: TCACCAAGTCCTTCCTGCCAGT R: CACAGCAGCCTGTGAACACCAG	105
GLUT8	Solute Carrier Family 2 Member 8	29988	F: GTCTCTGCACAGCCTGTTGATG R: GATCTCTGACATGAGGAGCCAG	126
GLUT10	Solute Carrier Family 2 Member 10	81031	F: GTGGAGATACGAGGAAGAGCCT R: TCAGTCCGTAGAGCAGGAAGGT	133
GLUT12	Solute Carrier Family 2	154091	F:	154

	Member 12		GCCACACTGAATACCAGATAGTC R: CCACCAGGAAAGATCTCGCTGA	
GLUT13	Solute Carrier Family 2 Member 13	114134	F: GTCTGGCTTGTTGAGAAGGTGG R: CGTTCTGACCTGACGGAGCTAT	157
GLUT14	Solute Carrier Family 2 Member 14	144195	F: CAATCGGCTCTTTCCAGTTTGGC R: CAAGGACCAGAGATTCGTGAGC	143
EGLN1	Egl-9 Family Hypoxia Inducible Factor 1	54583	F: GCCCAGTTTGCTGACATT R: CGTCTTTACCGACCGAAT	223
Actin	Actin, Beta	60	F: AGAGCTACGAGCTGCCTGAC R: AGCACTGTGTTGGCGTACAG	184

Table S2. Primers for ChIP and ReChIP

Name	Sequence	Product Size(bp)
GLUT1-TSS	F: GGACCGTAGCGTTTATAGGAC	176
	R: TGAGCGAGGCAGTGGTTAG	
SCD1-TSS	F: CCAATGACGAGCCGGAGTT	204
	R: AAGTGCGAGGAGTTGACTGG	
FADS2-TSS	F: CGGTGGGAGGAGTAGGAGAA	237
	R: CGCAGGTTATGCTTCTGAATCT	
LSH (site 1)	F: CACTAAAATGTCCGGGCGTG	152
	R: TAGGGTCTCACTCTGTCGTC	
LSH (Site 2)	F: ATTGGAGGTGGGAAAGGGAG	189
	R: TGGCCAGCAGAAGGAAGATT	

References

1. Shi Y, *et al.* Nuclear epidermal growth factor receptor interacts with transcriptional intermediary factor 2 to activate cyclin D1 gene expression triggered by the oncoprotein latent membrane protein 1. *Carcinogenesis* **33**, 1468-1478 (2012).

2. Jiang Y, *et al.* Repression of Hox genes by LMP1 in nasopharyngeal carcinoma and modulation of glycolytic pathway genes by HoxC8. *Oncogene* **34**, 6079-6091 (2015).

3. Dixon SJ, Stockwell BR. The role of iron and reactive oxygen species in cell death. *Nat Chem Biol* **10**, 9-17 (2014).

4. Dixon SJ, *et al.* Ferroptosis: an iron-dependent form of nonapoptotic cell death. *Cell* **149**, 1060-1072 (2012).